Published online 16 April 2007

Nucleic Acids Research, 2007, Vol. 35, No. 9 ***2913–2923***
doi:10.1093/nar/gkm115

Recruitment of DNA repair synthesis machinery to sites of DNA damage/repair in living human cells

Kazunari Hashiguchi[1], Yoshihiro Matsumoto[2] and Akira Yasui[1,*]

[1]Department of Molecular Genetics, Institute of Development, Aging and Cancer, Tohoku University, Sendai 980-8575, Japan and [2]Division of Medical Science, Fox Chase Cancer Center, PA 19111, USA

Received December 6, 2006; Revised February 3, 2007; Accepted February 8, 2007

ABSTRACT

The eukaryotic sliding DNA clamp, proliferating cell nuclear antigen (PCNA), is essential for DNA replication and repair synthesis. In order to load the ring-shaped, homotrimeric PCNA onto the DNA double helix, the ATPase activity of the replication factor C (RFC) clamp loader complex is required. Although the recruitment of PCNA by RFC to DNA replication sites has well been documented, our understanding of its recruitment during DNA repair synthesis is limited. In this study, we analyzed the accumulation of endogenous and fluorescent-tagged proteins for DNA repair synthesis at the sites of DNA damage produced locally by UVA-laser micro-irradiation in HeLa cells. Accumulation kinetics and *in vitro* pull-down assays of the large subunit of RFC (RFC140) revealed that there are two distinct modes of recruitment of RFC to DNA damage, a simultaneous accumulation of RFC140 and PCNA caused by interaction between PCNA and the extreme N-terminus of RFC140 and a much faster accumulation of RFC140 than PCNA at the damaged site. Furthermore, RFC140 knock-down experiments showed that PCNA can accumulate at DNA damage independently of RFC. These results suggest that immediate accumulation of RFC and PCNA at DNA damage is only partly interdependent.

INTRODUCTION

DNA replication and repair synthesis are essential cellular events in both prokaryotes and eukaryotes. Numerous reports have provided details of the nature of the chromosomal DNA replication machinery, which contains a sliding clamp and clamp loaders (1). The eukaryotic sliding DNA clamp, proliferating cell nuclear antigen (PCNA), is known to interact with many proteins related to DNA replication, DNA repair, translesion DNA synthesis, DNA methylation, cell cycle regulation, chromatin metabolism, sister chromatin cohesion and apoptosis, suggesting a central role in regulating normal cellular DNA replication/repair activities (2–4). PCNA is a ring-shaped homotrimer that encircles double-stranded DNA (dsDNA), leaving it free to slide along the DNA, and to function as a scaffold protein, interacting with many partners. The most important role of PCNA in DNA replication and repair is thought to be related to DNA polymerase processing, since PCNA interacts with multiple DNA polymerases and can stimulate their processivity (1,2,4,5).

Since PCNA is ring-shaped, it must be opened up to load onto DNA and closed following loading. Loading of PCNA onto DNA is performed by an ATP-dependent activity of Replication Factor C (RFC), a clamp loader complex consisting of five subunits: one large subunit p140 (Rfc1, RFC140) and four small subunits, p37 (Rfc2, RFC37), p36 (Rfc3, RFC36), p40 (Rfc4, RFC40) and p38 (Rfc5, RFC38). At initiation of DNA replication in eukaryotic cells, the DNA polymerase α-primase complex catalyzes the extension of DNA from 5′ to 3′. In this step, DNA polymerase α-primase does not require PCNA. After incorporation and polymerization of about 30 nt, this results in a 3′ template–primer junction. An *in vitro* study has revealed that the DNA-binding domain of RFC140 binds to this junction and helps to load PCNA onto DNA. DNA polymerase δ and/or ε are then recruited to PCNA, and begin the subsequent DNA synthesis (5,6).

RFC140 is a large subunit compared with the other four subunits. It has a BRCT domain (7,8) and an extended N-terminal domain (9), suggesting that RFC140 is more critical than the other small subunits. As mentioned earlier, RFC140 has a DNA-binding domain at a region between aa367 and 493. This region also contains a BRCT motif, which in a large number of proteins is involved in cell cycle regulation and DNA metabolism and has homology to bacterial DNA ligases and PARP, suggesting a role as a nick sensor (7,8). Based on this information, it is thought that this DNA-binding

*To whom correspondence should be addressed. Tel: +81-22-717-8465; Fax: +81-22-717-8470; Email: ayasui@idac.tohoku.ac.jp
Correspondence may also be addressed to Kazunari Hashiguchi. Tel: +81-22-717-8469; Fax: +81-22-717-8470; Email: hashiguchika@idac.tohoku.ac.jp

domain is important for recruitment, not only to DNA replication sites, but also to sites of DNA damage, because cells require replicative DNA polymerase δ for multiple DNA repair synthesis activities, including long-patch base excision repair, mismatch repair, nucleotide excision repair and double-strand break repair (2,3). Throughout these systems for recognition and excision of damage from DNA, initiation of repair is performed by specific repair proteins. After removing damage from DNA, the gapped DNA region must be filled in by DNA polymerase, and the nick sealed by DNA ligase. Thus, many spacio-temporally coordinated proteins are required to complete DNA repair. The *in vivo* dynamics of this process are not yet well-described, however.

Here, we have analyzed the recruitment of PCNA and RFC to sites of DNA damage/repair, in order to gain a better understanding of the mechanisms by which the proteins are recruited to these sites. We have developed a system for observing, *in situ*, the dynamics of DNA repair proteins as they respond to DNA damage induced by UVA-laser irradiation (10,11). Using a knock-down of RFC140, we show that recruitment of PCNA to sites of DNA damage is independent of RFC140. We then examine the PCNA-facilitated recruitment of deletion fragments of RFC140, showing its dependence on an interaction between PCNA and the extreme N-terminus of RFC140.

MATERIALS AND METHODS

Construction of expression vectors

pEGFP-C1 vector was purchased from Clontech, and its multi-cloning sites were slightly modified to introduce in-frame *Xho*I or *Sal*I and *Not*I sites (10,11). The coding regions of human RFC140, RFC40, RFC38, RFC37, RFC36, PCNA and DNA polδ-p125 were inserted into pEGFP-C1. Deletion fragments of RFC140 were PCR-amplified by oligonucleotide primers containing *Sal*I or *Not*I sites and inserted into pEGFP-C1 vector, in some cases using appropriate restriction endonucleases to generate constructs. Details are described in Supplementary Information. Site-directed mutagenesis was performed according to the QuikChange site-directed mutagenesis protocol (Stratagene). Sequences of all PCR primers used in this study can be provided upon request.

Antibodies

The antibodies used in indirect-immunofluorescent (IF) and Western (WB) experiments were as follows: rabbit polyclonal anti-RFC1 (diluted 1:100 for IF, 1:500 for WB, sc-20993, SantaCruz), rabbit polyclonal anti-PCNA (diluted 1:50 for IF, sc-7907, SantaCruz), mouse monoclonal anti-PCNA (PC10, diluted 1:100 for IF, 1:3000 for WB, NA03, Calbiochem), mouse monoclonal anti-phosphorylated H2AX (γH2AX, diluted 1:800 for IF, 05-636, Upstate), mouse monoclonal anti-ORC2 (diluted 1:3000 for WB, M055-3, MBL), mouse monoclonal anti-MEK2 (diluted 1:3000 for WB, 610235, BD Biosciences), goat polyclonal anti-Actin (diluted 1:3000 for WB, sc-1616, SantaCruz) and mouse monoclonal anti-His (diluted 1:2000 for WB, 27-4710-01, Amersham).

Cell culture and transfection

Wild-type and xrcc1-deficient mouse embryonic cells, having an inactive p53 background, were generous gifts of Samuel Wilson (NIEHS/NIH). These two lines, 293T and HeLa cells were cultured in Dulbecco's modified-MEM (Nissui) supplemented with 1 mM L-glutamine and 10% fetal bovine serum at 37°C and 5% CO_2. For UVA-laser irradiation, cells were seeded in glass-bottomed dishes (Matsunami Glass), and the GFP-expression vectors were transfected using FuGene6 (Roche) according to the manufacturer.

Microscopy and UVA-laser irradiation

Fluorescence images were obtained and processed using a FV-500 confocal scanning laser microscopy system (Olympus). UVA-laser irradiation using 365 and 405-nm wave-lengths was performed as described previously (10–12). The images obtained were processed by FluoView (Olympus) and Photoshop software.

Indirect immunofluorescence

Cells were plated in glass-bottomed dishes 2 days before experiments. Indirect immunofluorescence was performed as described previously (13), but with slight modification. Briefly, at appropriate time points after irradiation, cells were fixed with 4% paraformaldehyde and permeabilized with PBS/0.2% TritonX-100. Alternatively, for PCNA-staining, cells were first treated with detergent solution (10 mM Tris–HCl pH 7.5, 2.5 mM $MgCl_2$, 0.5% Nonidet P-40 and 1 mM PMSF) for 8 min on ice and fixed with ice-cold methanol. The secondary antibodies used were Alexa Fluor 488 anti-rabbit IgG and 594 anti-mouse IgG (diluted 1:400, Molecular Probes) as appropriate. All samples were counterstained with DAPI to ensure nuclear location.

Expression and purification of recombinant proteins

Escherichia coli BL21(DE3) pLysS (Invitrogen) was used as host strain for expression of recombinant proteins in this study. The coding region of the appropriate RFC140 fragments and human PCNA were inserted into pGEX-4T-3 (Amersham) and pET16b (Novagen), and expressed as GST- and His-tagged proteins, respectively.

When the bacterial culture had reached an OD_{600} of 0.6, expression of GST-RFC140 fragments was induced by addition of 1 mM IPTG and culture was continued at 23°C for 8 hr. In the case of His-PCNA, induction was by addition of 1 mM IPTG with further cultivation at 37°C for 3 hr. Bacteria were washed once with ice-cold PBS and stored at −80°C until use.

Cells expressing GST-RFC140 fragments were lyzed by two freeze-thaw cycles combined with sonication in Buffer A (50 mM Tris–HCl pH 8.0, 500 mM NaCl and 0.1% TritonX-100) supplemented with 1 mM DTT, Complete EDTA-free (Roche) and 1 mM PMSF. Lysates were clarified by centrifugation at 20 000 *g* for 30 min.

The supernatant was mixed with Glutathione Sepharose 4FF beads (Amersham) equilibrated with Buffer A supplemented with 1 mM DTT and incubated for 2 hr at 4°C with gentle rotation. Unbound proteins were washed out with Buffer A, and a portion of the beads was taken, mixed with SDS sample buffer, boiled and applied to SDS–PAGE to check the purity.

Cells expressing His-PCNA was lyzed by two freeze-thaw cycles combined with sonication in Buffer B (50 mM Tris–HCl pH 8.0, 500 mM NaCl, 0.1% TritonX-100 and 5 mM spermidine) supplemented with Complete EDTA-free, 1 mM PMSF and 20 mM imidazole. Lysates were clarified by centrifugation. The supernatant was mixed with Ni-NTA agarose resin (Qiagen) equilibrated with Buffer B supplemented with 20 mM imidazole and incubated for 2 hr at 4°C with gentle rotation. Unbound proteins were washed out with Buffer B containing 20 mM imidazole, and bound proteins were eluted with Buffer B containing 60, 100, 250 and 500 mM imidazole, sequentially. Most of the His-PCNA eluted in the 250 mM imidazole fraction.

GST-pull-down assay

The GST-pull-down assay was performed using GST-RFC140 fragments immobilized on glutathione sepharose resin as bait and a His-PCNA as prey. Immobilized GST (~2 μg) or GST-RFC140 fragments (~1 μg) were resuspended in Buffer C (40 mM Tris–HCl pH 7.5, 10 mM $MgCl_2$, 0.1% NP-40, 0.2% BSA) and 1 μg of His-PCNA was added. The mixture was incubated at room temperature for 1 hr with gentle rotation. Beads were then washed 4× in ice-cold Buffer C supplemented with 50 mM NaCl, and bound proteins were boiled in the presence of SDS-sample buffer and analyzed on a Western blot.

Chromatin fractionation

Cellular localization of endogenous RFC140 and PCNA in 293T cells was investigated by the chromatin fractionation technique according to the method of Mendez and Stillman (14), with slight modification. Briefly, 293T cells were plated in a 60-mm dish. At 80% confluence, cells were washed once in ice-cold PBS and the cell pellet was resuspended in 200 μl of Solution A (10 mM Hepes–KOH pH 7.9, 10 mM KCl, 1.5 mM $MgCl_2$, 0.34 M sucrose, Complete EDTA-free and 1 mM PMSF) and then TritonX-100 (0.1%) was added. After 5 min of incubation on ice, samples were centrifuged at 1300 *g* for 4 min (4°C). The resultant supernatant and pellet were designated as 'S1' and 'P1' fractions, respectively. The P1 fraction was washed once in Solution A, and this pellet was designated as 'P1 fraction (intact nuclei)'. Nuclei were resuspended in 200 μl of Solution B (3 mM EDTA and 0.2 mM EGTA) and left to stand on ice for 10 min. The sample was centrifuged at 1700 *g* for 4 min (4°C). The resultant supernatant and pellet were designated as 'S2' and 'P2', respectively. The 'P2' fraction was washed once with Solution B, and this pellet was designated as 'P2 fraction (chromatin)'. S1 and S2 fractions were centrifuged at 15 000 *g* for 5 min, and each supernatant was carefully transferred to a new tube, and designated as 'S1 (cytosol)' and 'S2 (soluble nuclear proteins)'. The P2 fraction was resuspended in 200 μl of SDS-sample buffer and sonicated. The same volumes of each of S1, S2 and P2 fractions were applied to SDS–PAGE, and proteins were blotted to a PVDF membrane. After staining with appropriate primary and secondary antibodies, proteins of interest were detected by ECL (Amersham).

siRNA transfections

Small interfering RNA (siRNA) oligonucleotides were prepared using a Silencer siRNA construction kit (Ambion) according to the manufacturer. The siRNA target sequences were as follows (sense strand only): RFC140 (GAAGGCGGCCUCUAAAUCA) (7); Luciferase (CGUACGCGGAAUACUUCGA). HeLa cells were plated at 1×10^5 per 35-mm dish and transfected twice with 100 nM siRNA using Oligofectamine (Invitrogen) on each of the following 2 days. The knock-down efficiency was evaluated by protein levels in whole cell extracts at 72 hr after the first siRNA transfection.

RESULTS

DNA repair synthesis machinery rapidly accumulates at DNA damage generated by UVA-laser irradiation of micro-nuclear regions

Our previous work showed that PCNA is rapidly recruited to sites of DNA damage induced by 365-nm UVA-laser irradiation (11). In this study, we have used primarily a 405-nm UVA-laser irradiation system. Using this approach, DNA damage, including single-strand breaks (SSBs), double-strand breaks (DSBs) and base damage, could be created along a single line. Our previous work (10) and Supplementary figure S1 showed that XRCC1-EGFP, EGFP-Rad52 and EGFP-OGG1 accumulate to a region irradiated by 405-nm UVA laser, suggesting that this laser irradiation induces SSBs, DSBs and base damage within a single region.

To determine whether the DNA repair synthesis machinery is recruited to sites of DNA damage, we transiently expressed EGFP-tagged RFC140, RFC40, RFC38, RFC37, RFC36, PCNA and the catalytic subunit of DNA polymerase δ p125 (Polδ1) in HeLa cells, and analyzed the dynamics of these fluorescence-tagged proteins, immediately following induction of damage, using confocal microscopy (Figure 1). The data clearly showed accumulation of all components tested. RFC began to accumulate immediately following irradiation (within 10 s), while the accumulation of PCNA and Polδ1 in the region of damage occurred somewhat later. A similar accumulation pattern was observed using 365-nm UVA-laser irradiation (Figure 2A) and the accumulation dynamics of EGFP-RFC140, PCNA and Polδ1 were also quantified (Figure 2B). Although PCNA and Polδ1 had similar accumulation kinetics, accumulation of RFC140 to the site of damage was much faster than for other proteins. This accumulation kinetics of RFC140 was co-plotted with that of the other four small subunits (Figure 2C). Since the difference in mean intensities of each subunit might be due to the differences in their

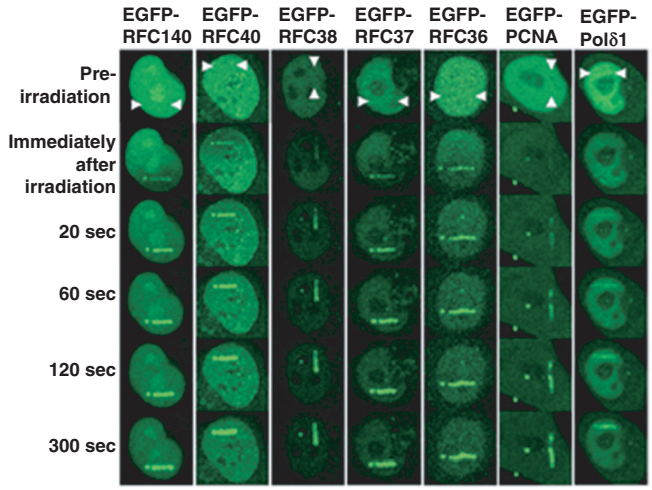

Figure 1. Recruitments of EGFP-tagged proteins related to DNA repair synthesis to laser-induced DNA damage. Five EGFP-fused RFC subunits, PCNA and catalytic subunit of DNA polδ (Polδ1) were transiently expressed in HeLa cells, and a 405-nm UVA-laser (500 scans) was directed to identical sites within nucleus (white arrowheads). The picture was taken before (pre-irradiation), immediately (within 10 s) and 20, 60, 120 and 300 s after irradiation.

expression levels, a time point at which 50% of maximum intensity was achieved (t 1/2 MI) was calculated from the data in Figure 2B and C (Figure 2D). The order of t 1/2 MI (fastest to slowest) was RFC140 ≫ RFC 38 > RFC 37 > RFC 40 > RFC 36 ≫ Polδ1 > PCNA. Although differences between the four small subunits of RFC were not apparent, these accumulated much more slowly than the large subunit RFC140. Furthermore, the accumulation of PCNA and Polδ1 was much slower than that of RFC140 (Figure 2B and D). This might indicate that RFC, especially RFC140, is recruited first to sites of DNA damage, and PCNA targets RFC for recruitment to sites of DNA damage.

Since these observations were made using over-expressed exogenous proteins, which may disrupt normal patterns of protein movement, we next examined the accumulation of endogenous RFC140 and PCNA to sites of DNA damage using indirect immunolabeling (Figure 3). For this experiment, phosphorylated H2AX (γH2AX) was probed as a marker of the laser-irradiated region. As shown, the pattern of accumulation kinetics for endogenous RFC140 and PCNA was quite similar to that of the EGFP-tagged proteins. The RFC140 signal was

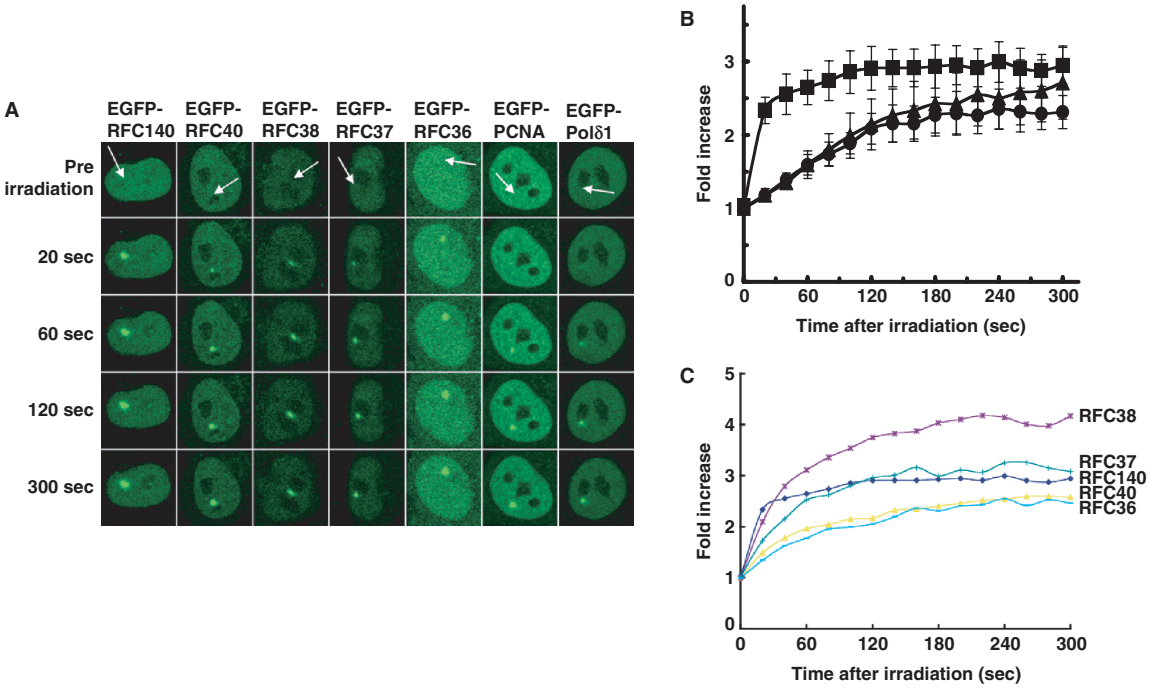

D

	RFC140	RFC40	RFC38	RFC37	RFC36	PCNA	Polδ1
MAX intensity (MI)	2.98	2.59	4.18	3.24	2.54	2.68	2.34
t MAX (sec)	239.68	260.00	219.96	239.69	239.66	300.60	240.88
1/2 MI	1.99	1.80	2.59	2.13	1.77	1.84	1.67
t 1/2 MI (sec)	13.08	41.89	32.89	38.51	57.71	85.31	73.85

Figure 2. (**A**) Recruitment of EGFP-tagged proteins related to DNA repair synthesis to DNA damage induced by a 365-nm UVA-laser. (A) Nuclei (arrowheads) of HeLa cells expressing EGFP-RFC140, EGFP-PCNA and EGFP-Polδ1, were irradiated with a 365-nm UVA laser as described in 'Materials and Methods' section. (**B**) Accumulation of EGFP-fusions, RFC140 (square), PCNA (triangle) and Polδ1 (circle) in (A) was measured as the fold increase of fluorescence intensity at an irradiated site. Data were taken from five independent experiments. Error bars represent standard errors. (**C**) Intensity at laser irradiation sites of EGFP-fusions and five RFC subunits was plotted as in (B). (**D**) Maximum intensity (MI) and the time to reach MI (t MAX) were represented in each GFP-fusion. A half of MI (1/2 MI) was calculated as $0.5 \times (\mathrm{MI} - 1) + 1$. Thus, t 1/2 MI indicates the time to reach 50% of MI.

strongest at 2 min after irradiation, and reduced with time until, 30 min after irradiation, most of this signal had disappeared. In contrast, the PCNA signal intensity peaked 5 min following irradiation, and was reduced thereafter. At 10 min following irradiation, although most of the RFC140 signal had disappeared, PCNA was retained, which is consistent with RFC140 releasing PCNA after loading it onto DNA. These data suggest that RFC140 accumulates at sites of DNA damage more rapidly than PCNA, as was seen in over-expressed proteins.

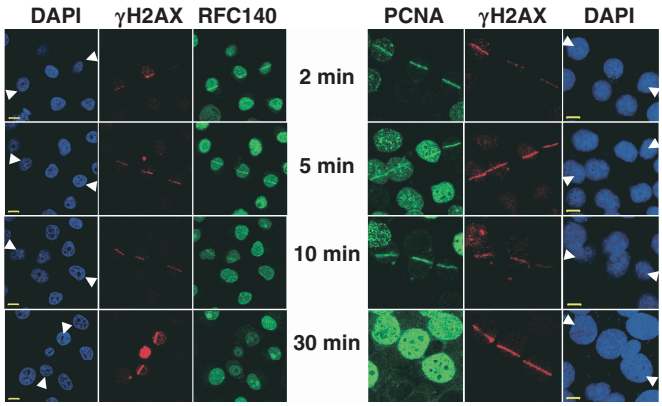

Figure 3. Recruitments of endogenous RFC140 and PCNA to laser-induced DNA damage. HeLa cells were plated in glass-bottomed dishes 2 days before irradiation, and cells were irradiated with a 405-nm UVA-laser at the positions indicated between the white arrowheads on the DAPI picture. At 2, 5, 10 and 30 min after irradiation, cells were fixed with paraformaldehyde (for RFC140) or methanol followed by detergent-treatment (for PCNA) and probed with anti-RFC140 or anti-PCNA antibody described in 'Materials and Methods' section. Phosphorylated H2AX (γH2AX) was the marker for showing actual laser irradiation.

As mentioned earlier, the 405-nm UVA-laser treatment apparently created both SSBs and DSBs. In our previous work (11), PCNA did not accumulate in xrcc1-deficient cells after a low dose of 365-nm irradiation that produced only SSBs, suggesting that PCNA accumulation to SSBs is dependent on XRCC1 protein. In that study, however, a high dose of 365-nm irradiation producing both SSBs and DSBs, caused accumulation of PCNA even in xrcc1-deficient cells, indicating that PCNA accumulation to DSB is independent of XRCC1. To explore the dependency of accumulation of RFC140 and PCNA on the nature of DNA damage, we expressed EGFP-fused RFC140 and PCNA in xrcc1-deficient and xrcc1-proficient MEF and irradiated with both low and high doses of 365-nm UVA-laser light. As shown in Figure 4, although both PCNA and RFC140 accumulated at SSBs in WT cells, neither protein did so in xrcc1-deficient cells. On the other hand, in the presence of a mixture of SSBs and DSBs, which is achieved by a higher dose of laser irradiation, within the irradiated region, both PCNA and RFC140 accumulated, regardless of the presence of XRCC1 protein in MEF. These data indicate that aspects of the XRCC1-dependency of RFC140 accumulation to DNA damage are similar to PCNA, suggesting accumulation of RFC140 to both SSBs and DSBs.

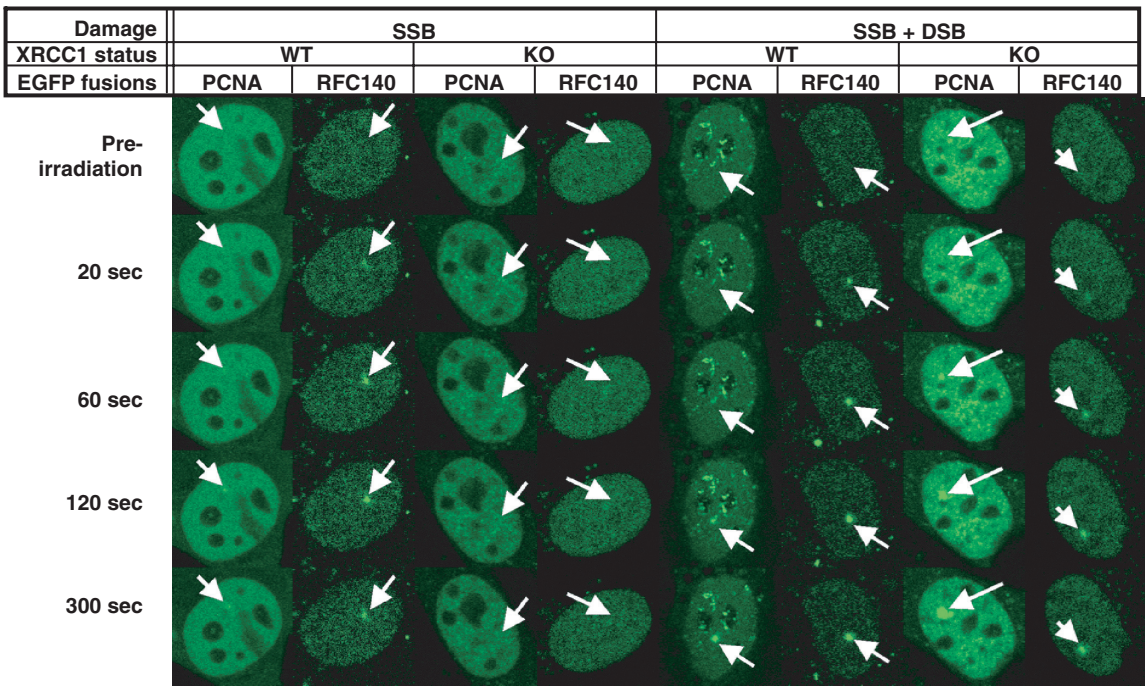

Figure 4. Accumulation of EGFP-RFC140 and EGFP-PCNA in response to laser-induced DNA damage in xrcc1-deficient and xrcc1-proficient mouse embryonic cells. Nuclei of xrcc1-deficient (KO) or proficient (WT) mouse embryonic cells expressing EGFP-RFC140 or EGFP-PCNA were irradiated with a low dose (SSBs) or a high dose (SSBs + DSBs) of 365-nm UVA-laser light. Time-lapse pictures were taken as indicated in Figure 2A.

Deletion analysis of RFC140 in accumulation at sites of DNA damage

Based on the above results, we hypothesized that RFC140 accumulates at sites of damage first and then recruits PCNA. To test this hypothesis we determined which parts of RFC140 are important for the protein to accumulate at sites of DNA damage. We generated a series of GFP-tagged RFC140 fragments based on the physical domains of RFC140 as shown in Figure 5A: PCNA-A and PCNA-B domains which are thought to be critical for PCNA-binding, a DNA-binding domain which has affinity to 3′ template–primer junction generated by Pol α-primase, and a complex-formation domain that is required for complex formation with other RFC subunits (7). We first tested two fragments: the N-terminal half (fragment 1–493) and the C-terminal half (fragment 480–1147) of RFC140. Both fragments showed exclusively nuclear localization and localized to sites of DNA damage after local UVA-laser irradiation. However, fragment 1–493 showed much stronger accumulation than fragment 480–1147 (Figure 5A and B).

In addition, fragments 480–882 and 734–1147 from the C-terminal half, and fragments 1–369 and 367–493 from the N-terminal half were created (Figure 5A). Of these four fragments, only fragments 1–369 and 480–882, containing the PCNA-binding domain, localized to the nucleus. The complex-formation domain-containing fragment (734–1147) localized only in the cytosol (data not shown). The fragment containing the DNA-binding domain (367–493) localized throughout whole cells (data not shown), which is consistent with the previous data by Fotedar and co-workers (15). In the present study, the complex formation domain and DNA-binding domain were fused with artificial 2xNLS (nuclear localization signal) as shown in Figure 5A. After addition of the NLS, both fragments showed nuclear localization (Figure 5B).

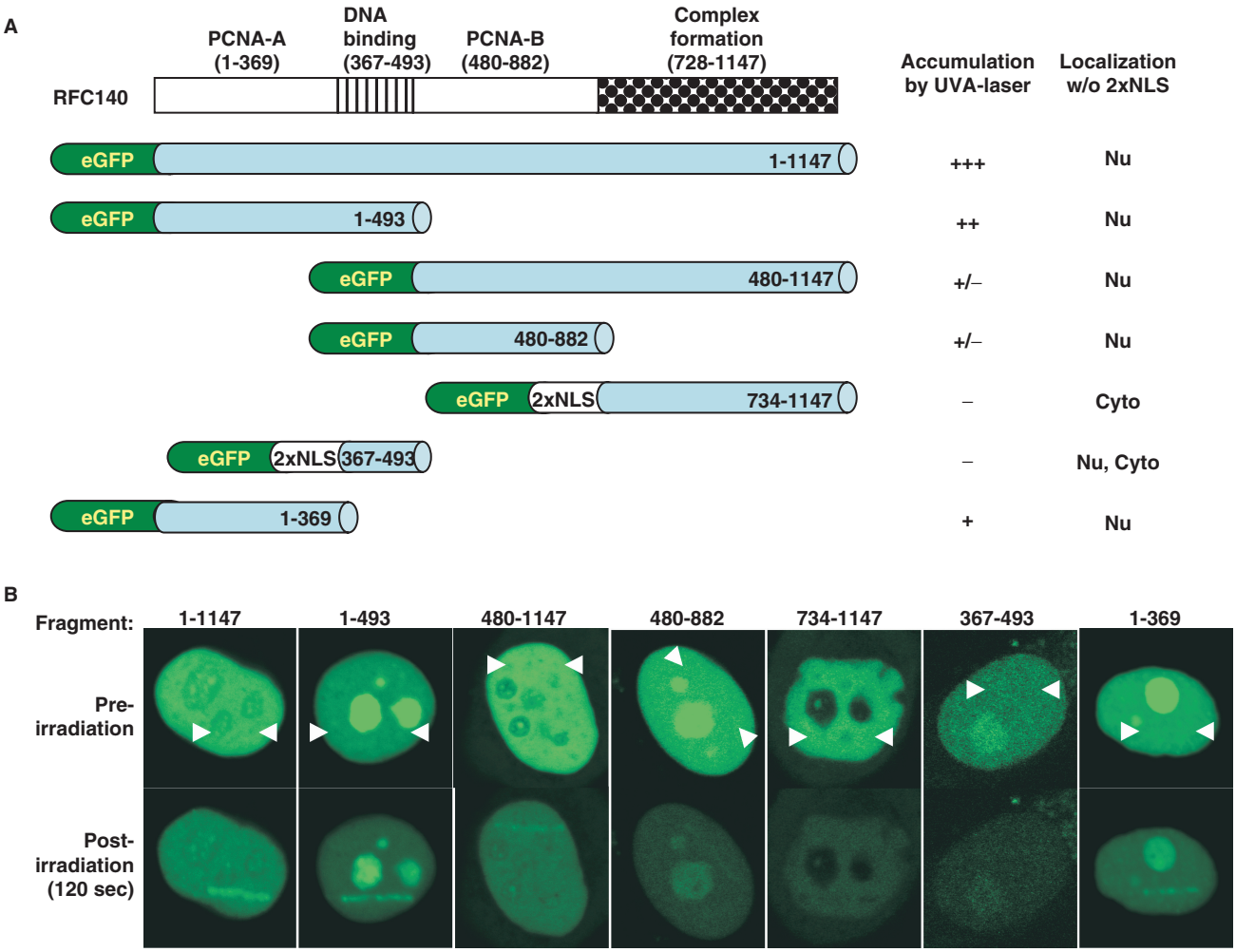

Figure 5. Deletion analysis of RFC140. (**A**) The domain structure of RFC140 and RFC140 fragments. Details of each domain are described in the text. The degree of accumulation of each fragment at laser-induced DNA damage is indicated as follows: +++, accumulation of full-length protein (as 100% when 120 s after irradiation); ++, weaker accumulation of full-length (more than 70%); +, much weaker accumulation of full-length (30–70%); +/−, very weak accumulation (less than 30%) and -, no accumulation. Localization of each EGFP-fragment without 2xNLS is also indicated. Nu and Cyto indicate nuclear and cytosolic localization, respectively. (**B**) Accumulation of each EGFP-fragment is shown at 120 s time point after irradiation.

Of these four fragments, the DNA-binding domain and complex-formation domain did not accumulate (Figure 5B). The other two PCNA binding fragments showed accumulation with different strengths; fragment 1–369 showed much more significant accumulation than fragment 480–882. This might indicate that RFC140 accumulates to sites of DNA damage by binding to PCNA, and that two distinct regions for PCNA-binding have different properties.

Effect of F6A/F7A mutation in deletion fragments on accumulation at DNA damage

To determine whether accumulation of fragment 1–369 is PCNA-dependent, we introduced two phenylalanine-to-alanine substitutions at aa 6 and 7 (F6A/F7A) in fragment 1–369 (Figure 6A) (designated as fragment 1–369FA) since RFC140 contains a PCNA-binding motif (PIP-box) at its N-terminus (2) which is thought to be responsible for the interaction of PCNA with this fragment (9). Interestingly, fragment 1–369FA showed neither exclusive nuclear localization nor accumulation at the site of DNA damage (Figure 6B). This data suggested that nuclear localization of fragment 1–369 requires an efficient interaction with PCNA and the presence in nucleus of this fragment is important for accumulation at DNA damage. This is distinct from the model developed earlier.

To evaluate the extent to which PCNA is responsible for accumulation of RFC140, deletion fragments having normal (wild-type) or F6A/F7A substitution were constructed, and their accumulation kinetics quantified (Figure 6C–F). Surprisingly, fragment 1–397FA localized exclusively in the nucleus and accumulated at laser-irradiated sites (Figure 6C), although this fragment was extended by only 28 C-terminal aa compared with fragment 1–369FA. However, the accumulation kinetics of fragment 1–397FA were completely different from its wild-type version (Figure 6C). Immediately after irradiation, accumulation of fragment 1–397 F6A/F7A reached a plateau; however the wild-type fragment continued to accumulate. The same pattern was seen with fragments 1–493FA and 1–733FA (Figure 6D and E). To ensure PCNA binding ability in mutant fragments, we did a GST-pull-down assay using GST–RFC fragments and His-PCNA as bait and prey, respectively (Figure 7). Compared with fragments 1–369WT and 1–369FA, PCNA binding ability was markedly decreased in fragment 1–369FA. The same pattern was observed in fragments 1–397WT and 1–397FA. Although some of bound PCNA could be seen in fragments 1–369FA and 1–397FA, it seems that this residual binding is caused by the more amounts of bait protein (GST-fusion) in FA fractions compared within WT fractions. Furthermore, the GST-tag fused to N-terminal RFC140 fragments might affect on stability of protein interaction in this case, because the FA mutation is located at very extreme N-terminus of fragments. Thus, since the binding activities in fragments 1–369FA and 1–397FA were not significant, it is thought that accumulation of fragment 1–397FA is independent of PCNA.

Accumulation of the full-length fragment also followed a similar kinetic pattern as the others (Figure 6F). Again, accumulation of all fragments with the F6A/F7A mutation reached a plateau soon after irradiation. On the other hand, recruitment of wild-type fragments increased with time. These results clearly indicated the importance of an interaction with PCNA at the N-termini for accumulation of RFC140 to DNA damage. Although fragment 1–1147FA showed inefficiency in the slower phase of accumulation, this accumulation may also be meaningful. These results suggest that a slower phase of RFC140 accumulation to the site of DNA damage is due to binding to PCNA and its rapid phase is via a short region of RFC140, including at least aa 370–397.

It should be noted that fragment 1–733FA, like fragment 1–397FA, did not accumulate further after 40 s, although another PCNA-binding domain (PCNA-B domain) was still active in fragment 1–733FA (Figure 6C and E). On the other hand, fragment 480–733 which contains the PCNA-B domain had far greater interaction ability than the PCNA-A domain *in vitro* (Figure 7). Since the PCNA-B domain (fragment 480–882) showed very slight accumulation compared with the PCNA-A domain (fragment 1–369) (Figure 5), these data also support the importance of interaction with PCNA via the A domain but not via the B domain for accumulation of RFC140 to DNA damage.

Sub-cellular localization of endogenous RFC140 and PCNA

In order to investigate the sub-cellular localization of endogenous RFC140 and PCNA in asynchronous cells, we next prepared cytoplasmic (S1), soluble (S2) and insoluble (P2) nuclear protein fractions from 293T cells. With this procedure, the soluble (S2) and insoluble (P2) nuclear fractions are thought to be the nucleoplasm and the chromatin/nuclear matrix, respectively (14). As shown in Figure 8, ORC2, which is a marker protein tightly bound to chromatin is completely absent from the S2 fraction confirming that S2 does not contain any contaminating P2 fraction so it should not contain chromatin-binding proteins. The presence of endogenous RFC140 in the P2 fraction but not the S2 from 293T cells shows that it is purely a chromatin-binding protein, whereas PCNA was found throughout all the sub-cellular fractions (Figure 8). This different distribution of these proteins might be explained by the more rapid recruitment of RFC140 than PCNA to site of DNA damage.

Accumulation of PCNA is not dependent on RFC140

To evaluate the inter-dependency of PCNA and RFC140 on each others' accumulation, we used siRNA-mediated knock-down of the proteins in HeLa cells. Unfortunately, however, knock-down of PCNA was inefficient (data not shown), so we could only perform this experiment with RFC140 (Figure 9A). HeLa cells were transfected with siRNA, cells were fixed at 2 and 5 min after UVA-laser irradiation, and accumulation of endogenous RFC140 and PCNA was observed by indirect-immunolabeling (Figure 9B). Accumulation of

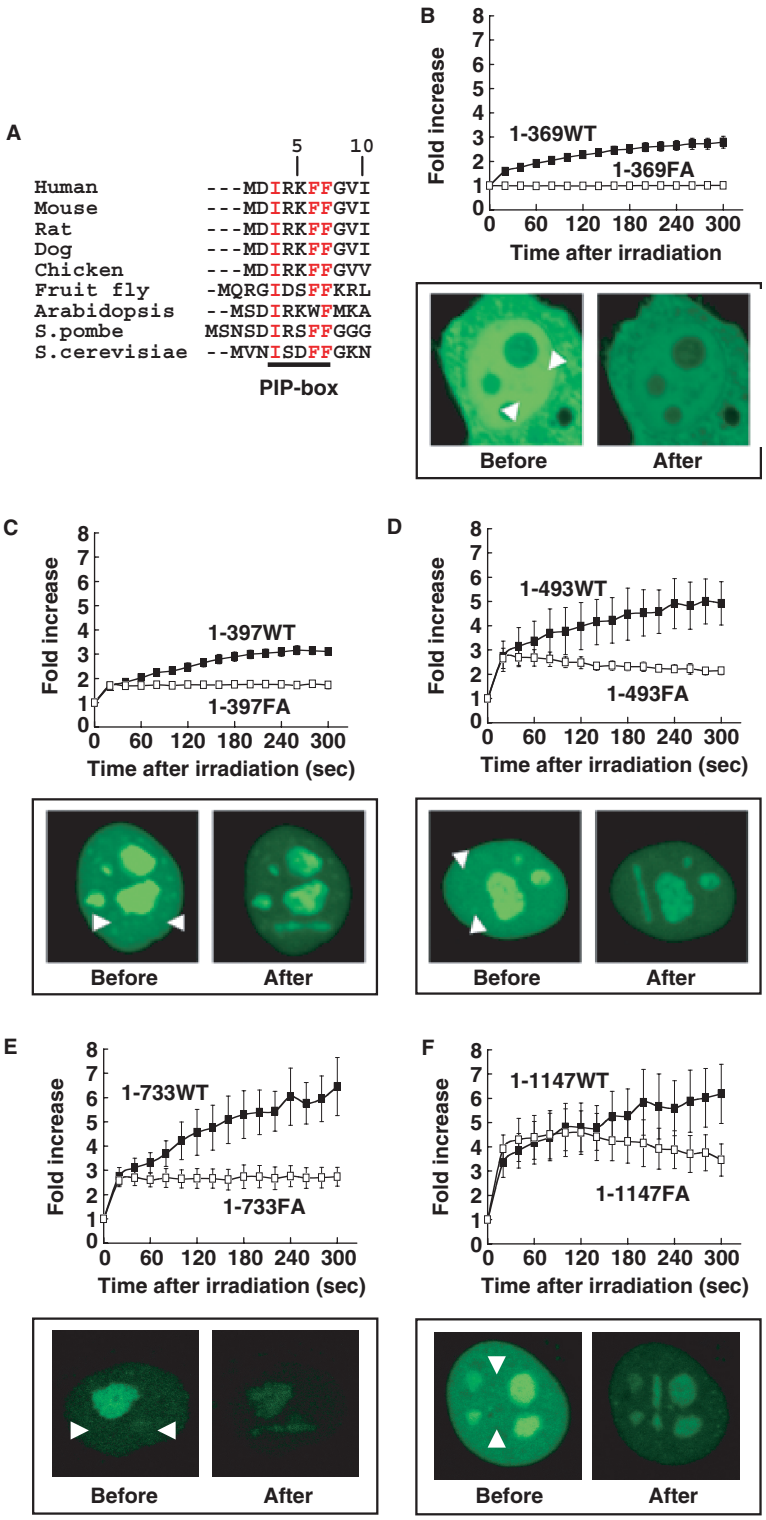

Figure 6. Accumulation kinetics of a series of deletion fragments with or without F6A/F7A substitution. (**A**) Sequence alignment of the N-terminal portion of RFC140 orthologs from nine eukaryotes. Approximately 10 amino-acid residues are indicated. Red-colored residues are highly conserved among all species, and are indicated as the PIP-box (see text). EGFP-fused fragments 1–369 (**B**), 1–397 (**C**), 1–493 (**D**), 1–733 (**E**) and full-length (1–1147, **F**) having normal (closed squares) or the F6A/F7A mutation (open squares) were transiently expressed in HeLa cells and accumulation was measured as the fold increase of fluorescence intensity. Error bars indicate standard error. Error bars not indicated are smaller than symbols. Pictures represent accumulation of FA mutant fragments, and are taken before and 120 min after laser irradiation. Data were taken from five independent experiments. White arrowheads indicate the laser irradiation region.

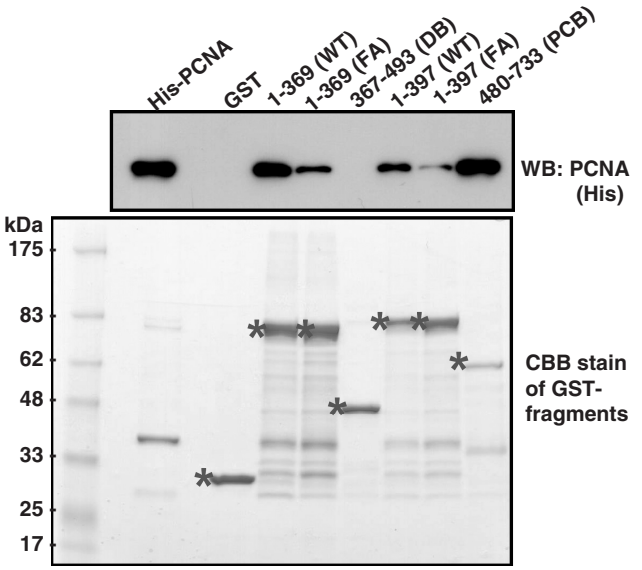

Figure 7. GST-pull-down assay. GST-fused RFC140 fragments were purified and indicated as asterisks on Coomassie staining gel (bottom column). GST-fragments immobilized on glutathion sepharose beads were mixed with purified His-PCNA, and GST-pull-down assay was done as described in 'Materials and Methods' section. On the His-PCNA lane, 10% of input protein was loaded. Bound PCNA was detected by Western blots with anti-His antibody (top column).

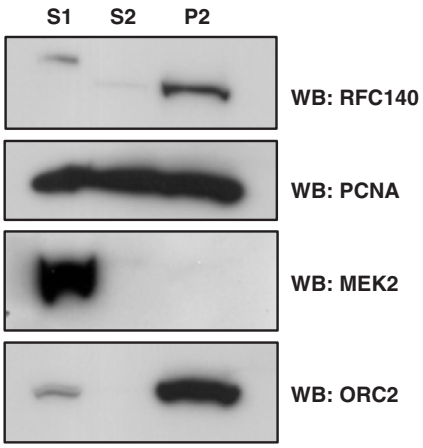

Figure 8. Cellular localization of endogenous RFC140 and PCNA in asynchronous 293T cells. S1, S2 and P2 indicate cytoplasmic, nucleoplasm (soluble nuclear) and chromatin/nuclear matrix (insoluble nuclear) fractions, respectively. MEK2 and ORC2 blots are represented as a markers specific to cytoplasmic and chromatin fractions, respectively.

PCNA and RFC140 was observed in cells treated with control siRNA (Luciferase siRNA) (Figure 9B, indicated as siLuc). In the cells treated with RFC140 siRNA, PCNA still accumulated at sites of damage, even in the absence of RFC140 protein (Figure 9B, indicated as siRFC140 column). This indicates that PCNA accumulates at DNA damage and that its accumulation is independent of RFC140.

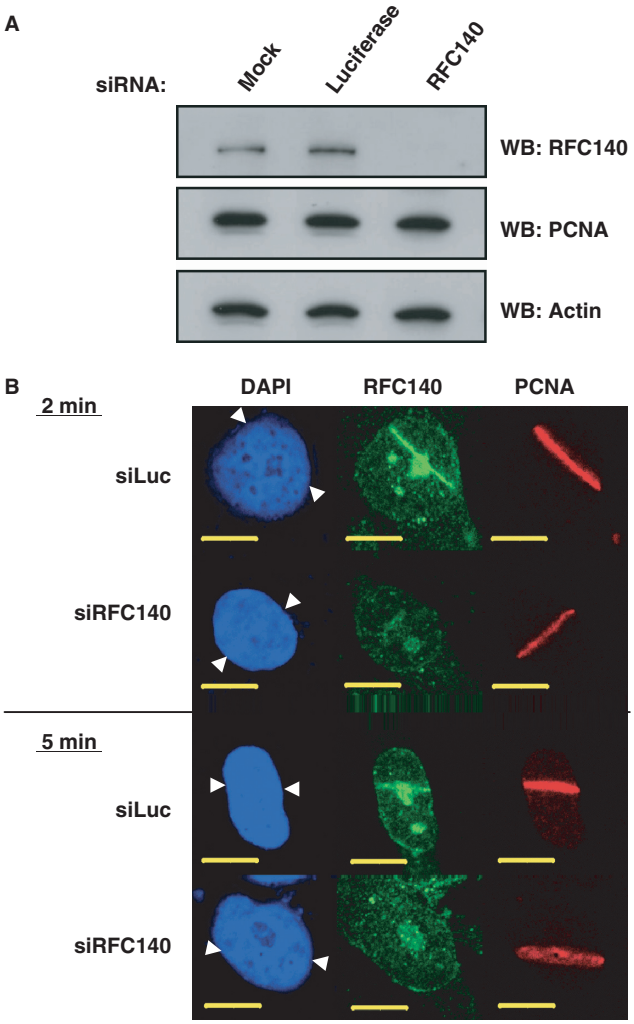

Figure 9. Effect of absence of RFC140 on accumulation of PCNA at DNA damage. (**A**) siRNA-mediated RFC140 knock-down. Whole cell extracts were prepared from mock-, Luciferase siRNA- and RFC140 siRNA-treated HeLa cells as described in 'Materials and Methods' section. Blot was probed with anti-RFC140, PCNA and Actin antibodies. (**B**) Indirect immunofluorescence. Luciferase siRNA- and RFC140 siRNA-treated HeLa cells were irradiated with a 405-nm UVA-laser and fixed at 2 or 5 min after irradiation. Indirect immunolabeling was performed as described in 'Materials and Methods' section.

DISCUSSION

In this study, we first of all clearly demonstrated rapid recruitment (within 2 min of damage induction) of PCNA, DNA Polδ1 and all subunits of RFC as exogenous EGFP-fusions, and of PCNA and RFC140 as endogenous proteins, to the sites of DNA damage induced by UVA-laser irradiation of living cells. To further understand the mechanisms of recruitment to sites of DNA damage, a series of fragments and point mutants of RFC140 were investigated, because the accumulation of EGFP epitope-tagged RFC 140 was apparently faster than that of EGFP-PCNA (Figures 1 and 2), which suggested that RFC may recruit PCNA to the sites of DNA damage. Differential accumulation of fragments 1–369WT and 1–369FA

showed that accumulation of this region is totally dependent on exclusive nuclear localization of those fragments (Figure 6B). Although full-length RFC140 containing the F6A/F7A substitution could accumulate, this mutant fragment showed inefficiency in the slower phase of accumulation (Figure 6F), suggesting dependency of RFC140 accumulation on the exclusive nuclear localization via binding with PCNA. A RFC140 siRNA-mediated knock-down revealed that PCNA accumulates at DNA damage independently of the presence of RFC140 (Figure 9). These results indicate that the major pathway in recruitment of PCNA and RFC is due to targeting of PCNA to the site of DNA damage/repair. In support of this, when SSBs are induced, PCNA is thought to be recruited to DNA damage sites through interaction with XRCC1 (11), probably by direct interaction between XRCC1 and PCNA (16). Furthermore, a very recent report by Das-Bradoo and co-workers (17) suggests that, in budding yeast, Polα interacts with Mcm10 and diubiquitinated Mcm10 interacts with PCNA, allowing recruitment of PCNA to sites of DNA replication. These data may indicate that PCNA is targeted to sites of DNA replication/repair without RFC. In addition, the PIP-boxes in several PCNA-binding proteins are required for DNA metabolism which relates to recruitment of these proteins. Recruitment of DNA methyltransferase I to sites of DNA damage (18), of RFC140 and DNA ligase I to DNA replication sites (19) and of DNA ligase I to DNA repair sites (20) required a PCNA-binding domain. Therefore, the accumulation of fragment 1–369WT but not 1–369FA to the sites of DNA damage/repair might be by a similar mechanism to that indicated above and, furthermore, RFC might be recruited to the sites of DNA damage/repair as a co-factor of PCNA. However, PCNA-dependent accumulation of RFC140 was unexpected, because, in our hands, the DNA-binding domain, which has the ability to 'find' DNA replication sites (5), did not show accumulation (Figure 5). This domain is probably required for a later step, i.e. locating accumulated PCNA for accurate loading within DNA damage/repair sites.

However, surprisingly, the accumulation of EGFP-tagged RFC140 was apparently much faster than for EGFP-tagged PCNA (Figure 2B). From the data shown in Figure 6, there is no doubt that RFC140 also has a PCNA-independent accumulation property, even if this is a minor one compared to its PCNA-dependent accumulation. In spite of the presence of only extra 28 aa in fragment 1–397 compared with fragment 1–369, mutant type of this fragment (1–397FA) showed exclusive nuclear localization, even if fragment 1–369FA was not (Figure 6B and C). However we could not find any NLS in this region (aa369–397) by the PSORTII prediction (data not shown). This information gave us the following idea. This extra 28 aa might contain a cryptic NLS ability and contribute to the exclusive nuclear localization of RFC140. Once fragments import to nucleus, those fragments can accumulate at DNA damage sites, suggesting that efficient PCNA binding is not required for this event. Although the role and mechanism of this faster accumulation of RFC140 than that of PCNA is still unclear, our subcellular localization study revealed that endogenous RFC140 is solely a chromatin-binding protein, whereas PCNA was distributed in both soluble and chromatin fractions in asynchronous 293T cells (Figure 8). Zou and co-workers (21) reported that Rad17, which is a checkpoint protein and one of the RFC140 homologs that loads the Rad9-Hus1-Rad1 clamp onto DNA, was found in both soluble and chromatin fractions, and did not change its localization status even after induction of DNA damage. Therefore it is possible that the immediate accumulation of RFC140 (PCNA-independent accumulation) may occur by the protein sliding along the chromatin and being trapped at sites of DNA damage. We propose the following model: since a certain proportion of PCNA is localized in the soluble fraction (Figure 8), it may be recruited to DNA damage with or without RFC140 (from the data shown in Figure 9B); some of the PCNA may encounter RFC140 at sites of damage, after which PCNA is loaded onto DNA by RFC. Thus our data strongly suggest that RFC140 has two distinct modes of accumulation to the sites of DNA damage/repair, PCNA-dependent and PCNA-independent.

The crystal structure of yeast RFC140 has been investigated for fragments 295–785 (corresponding to 568–1076 in the human protein) (22). Although this region contains a PCNA-binding domain, another PCNA-binding region located at the extreme N-terminus is lacking. Our study showed that fragment 1–369 (containing a PCNA-A binding domain) has much greater accumulation properties than fragment 480–1147 (containing a PCNA-B binding domain) (Figure 5), and the PCNA-A binding domain might have a more important role in the interaction with RFC140 than the PCNA-B binding domain (Figure 6E). However, the spatial location of these two distinct regions within the full-length protein may further stabilize the interaction with PCNA. Gomes and co-workers (23) investigated the phenotype of the yeast RFC140 fragment 274–861 (corresponding to 535–1147 in human). They revealed that yeast cells having deletion fragment 274–861 show a normal response to UV and hydroxyurea, but are sensitive to MMS compared with wild-type cells. This might indicate that the N-terminal portion of RFC140 is responsible for repair of MMS-induced strand breaks, but not for DNA replication or repair of UV-induced DNA damage. Together with this evidence, it might be suggested that the N-terminal portion of RFC140 is important for the interaction with PCNA in response to DNA strand breaks.

In summary, together with the previous studies, our model of the recruitment of the DNA repair synthesis machinery to sites of DNA damage/repair in living cells is as follows: after or during excision of damaged DNA from the genome, the PCNA/RFC complex is recruited to sites of DNA damage (Figures 1–4). At this time, it is PCNA that locates the sites of DNA damage rather than RFC (Figure 9). Prior to the translocation of the PCNA/RFC complex, RFC140 interacts with PCNA through the extreme N-terminal domain (PCNA-A domain) of RFC140 (Figures 5 and 6B); this interaction may be especially important in the response to DNA strand-breaks (23). After this interaction, an additional

interaction between PCNA and the PCNA-B domain of RFC140 may stabilize the PCNA/RFC complex [Figure 7 and (15)]. After accumulation of the PCNA/RFC complex, the DNA-binding domain of RFC140 locates the precise place where PCNA should be loaded [suggested in (8) and (15)]. RFC is then released from PCNA and DNA polδ is recruited to PCNA for DNA repair synthesis (24). In this study, again, it is strongly suggested that PCNA but not RFC is first recruited to the sites of DNA damage/repair, and RFC which is a 'co-factor' of PCNA loads PCNA onto the precise sites of DNA damage/repair. As mentioned earlier, RFC140 may accumulate rapidly at the damage site, although this mechanism and its significance are not yet resolved. However, our data suggest that RFC140 may have additional function(s) in DNA damage sensing that is independent of RFC's other small subunits (Figure 2). The data shown in Figure 4 and our previous data (11), strongly suggest that XRCC1 is the major recruiter of PCNA to SSBs. The next goal of this project will be to determine what is the PCNA recruiter for other types of DNA damage, i.e. DSBs. We anticipate that the laser microirradiation system will be a powerful tool for achieving this aim.

SUPPLEMENTARY DATA

Supplementary data are available at NAR online.

ACKNOWLEDGEMENTS

We are grateful to Samuel Wilson (NIEHS/NIH) for providing the wild-type and xrcc1-deficient cell lines. This work was supported in part by a grant of the Genome Network Project and by Grant-in-Aid for Scientific Research 18012003 from the Ministry of Education, Culture, Sports, Science and Technology, Japan (to A.Y.). Funding to pay the Open Access publication charge was provided by the Genome Network Project.

Conflict of interest statement. None declared.

REFERENCES

1. Johnson,A. and O'Donnell,M. (2005) Cellular DNA replicases: components and dynamics at the replication fork. *Annu. Rev. Biochem.*, **74**, 283–315.
2. Maga,G. and Hubscher,U. (2003) Proliferating cell nuclear antigen (PCNA): a dancer with many partners. *J. Cell Sci.*, **116**, 3051–3060.
3. Warbrick,E. (2000) The puzzle of PCNA's many partners. *Bioessays*, **22**, 997–1006.
4. Prosperi,E. (2006) The fellowship of the rings: distinct pools of proliferating cell nuclear antigen trimer at work. *FASEB J.*, **20**, 833–837.
5. Majka,J. and Burgers,P.M. (2004) The PCNA-RFC families of DNA clamps and clamp loaders. *Prog. Nucleic Acid Res. Mol. Biol.*, **78**, 227–260.
6. Maga,G., Stucki,M., Spadari,S. and Hubscher,U. (2000) DNA polymerase switching: I. Replication factor C displaces DNA polymerase alpha prior to PCNA loading. *J. Mol. Biol.*, **295**, 791–801.
7. Anderson,L.A. and Perkins,N.D. (2003) Regulation of RelA (p65) function by the large subunit of replication factor C. *Mol. Cell. Biol.*, **23**, 721–732.
8. Kobayashi,M., Figaroa,F., Meeuwenoord,N., Jansen,L.E. and Siegal,G. (2006) Characterization of the DNA binding and structural properties of the BRCT region of human replication factor C p140 subunit. *J. Biol. Chem.*, **281**, 4308–4317.
9. Venclovas,C., Colvin,M.E. and Thelen,M.P. (2002) Molecular modeling-based analysis of interactions in the RFC-dependent clamp-loading process. *Protein Sci.*, **11**, 2403–2416.
10. Lan,L., Nakajima,S., Komatsu,K., Nussenzweig,A., Shimamoto,A., Oshima,J. and Yasui,A. (2005) Accumulation of Werner protein at DNA double-strand breaks in human cells. *J. Cell Sci.*, **118**, 4153–4162.
11. Lan,L., Nakajima,S., Oohata,Y., Takao,M., Okano,S., Masutani,M., Wilson,S.H. and Yasui,A. (2004) In situ analysis of repair processes for oxidative DNA damage in mammalian cells. *Proc. Natl. Acad. Sci. USA*, **101**, 13738–13743.
12. Karmakar,P., Seki,M., Kanamori,M., Hashiguchi,K., Ohtsuki,M., Murata,E., Inoue,E., Tada,S., Lan,L. *et al.* (2006) BLM is an early responder to DNA double-strand breaks. *Biochem. Biophys. Res. Commun.*, **348**, 62–69.
13. Okano,S., Lan,L., Caldecott,K.W., Mori,T. and Yasui,A. (2003) Spatial and temporal cellular responses to single-strand breaks in human cells. *Mol. Cell Biol.*, **23**, 3974–3981.
14. Mendez,J. and Stillman,B. (2000) Chromatin association of human origin recognition complex, cdc6, and minichromosome maintenance proteins during the cell cycle: assembly of prereplication complexes in late mitosis. *Mol. Cell Biol.*, **20**, 8602–8612.
15. Fotedar,R., Mossi,R., Fitzgerald,P., Rousselle,T., Maga,G., Brickner,H., Messier,H., Kasibhatla,S., Hubscher,U. and Fotedar,A. (1996) A conserved domain of the large subunit of replication factor C binds PCNA and acts like a dominant negative inhibitor of DNA replication in mammalian cells. *EMBO J.*, **15**, 4423–4433.
16. Fan,J., Otterlei,M., Wong,H.K., Tomkinson,A.E. and Wilson,D.M.3rd. (2004) XRCC1 co-localizes and physically interacts with PCNA. *Nucleic Acids Res.*, **32**, 2193–2201.
17. Das-Bradoo,S., Ricke,R.M. and Bielinsky,A.K. (2006) Interaction between PCNA and Diubiquitinated Mcm10 is essential for cell growth in budding yeast. *Mol. Cell Biol.*, **26**, 4806–4817.
18. Mortusewicz,O., Schermelleh,L., Walter,J., Cardoso,M.C. and Leonhardt,H. (2005) Recruitment of DNA methyltransferase I to DNA repair sites. *Proc. Natl. Acad. Sci. USA*, **102**, 8905–8909.
19. Montecucco,A., Rossi,R., Levin,D.S., Gary,R., Park,M.S., Motycka,T.A., Ciarrocchi,G., Villa,A., Biamonti,G. and Tomkinson,A.E. (1998) DNA ligase I is recruited to sites of DNA replication by an interaction with proliferating cell nuclear antigen: identification of a common targeting mechanism for the assembly of replication factories. *EMBO J.*, **17**, 3786–3795.
20. Mortusewicz,O., Rothbauer,U., Cardoso,M.C. and Leonhardt,H. (2006) Differential recruitment of DNA Ligase I and III to DNA repair sites. *Nucleic Acids Res.*, **34**, 3523–3532.
21. Zou,L., Cortez,D. and Elledge,S.J. (2002) Regulation of ATR substrate selection by Rad17-dependent loading of Rad9 complexes onto chromatin. *Genes Dev.*, **16**, 198–208.
22. Bowman,G.D., O'Donnell,M. and Kuriyan,J. (2004) Structural analysis of a eukaryotic sliding DNA clamp-clamp loader complex. *Nature*, **429**, 724–730.
23. Gomes,X.V., Gary,S.L. and Burgers,P.M. (2000) Overproduction in Escherichia coli and characterization of yeast replication factor C lacking the ligase homology domain. *J. Biol. Chem.*, **275**, 14541–14549.
24. Podust,V.N., Tiwari,N., Stephan,S. and Fanning,E. (1998) Replication factor C disengages from proliferating cell nuclear antigen (PCNA) upon sliding clamp formation, and PCNA itself tethers DNA polymerase delta to DNA. *J. Biol. Chem.*, **273**, 31992–31999.